International Communications in Heat and Mass Transfer 119 (2020) 104980

Contents lists available at ScienceDirect

International Communications in Heat and Mass Transfer

journal homepage: www.elsevier.com/locate/ichmt

Entropy analysis in the Rabinowitsch fluid model through inclined Wavy Channel: Constant and variable properties

Yu-Ming Chu[a,b], Mubbashar Nazeer[c], M. Ijaz Khan[d], Waqas Ali[e], Zareen Zafar[i], Seifedine Kadry[f], Zahra Abdelmalek[g,h,*]

[a] Department of Mathematics, Huzhou University, Huzhou 313000, PR China
[b] Hunan Provincial Key Laboratory of Mathematical Modeling and Analysis in Engineering, Changsha University of Science and Technology, Changsha 410114, PR China
[c] Department of Mathematics, Institute of Arts and Sciences, Government College University Faisalabad, Chiniot Campus 35400, Pakistan
[d] Department of Mathematics and Statistics, Riphah International University, I-14, Islamabad 44000, Pakistan
[e] Chair of Production Technology, Faculty of Engineering Technology, University of Twente, the Netherlands
[f] Department of Mathematics and Computer Science, Beirut Arab University, Beirut, Lebanon
[g] Institute of Research and Development, Duy Tan University, Da Nang 550000, Viet Nam
[h] Faculty of Medicine, Duy Tan University, Da Nang 550000, Viet Nam
[i] Department of Mathematics, Riphah International University, Faisalabad Campus, Faisalabad 38000, Pakistan

ARTICLE INFO

Keywords:
Entropy generation
Rabinowitsch fluid
Inclined wavy channel
Peristalsis
Constant and variable properties

ABSTRACT

Entropy production in a system affects the efficiency of the system because it minimizes the output of the system. For the better performance of the system, it is very important to minimize the entropy production. Entropy generation is always observed in any irreversible process while it remains constant in any reversible process. Second law of thermodynamics play an important in the optimization of entropy generation rate. The main objective of this investigation is to minimize the entropy production through an inclined channel filled with Rabinowitsch fluid. For the better results, we will visually show the entropy generation under the account of two different cases. In the first case, we will choose the viscosity and thermal conductivity of the fluid as a constant and for the second case, viscosity and thermal conductivity will be treated as a variable. Further, the comparison of both the cases will be given under the effects of fluidic parameters. The Exact solutions of velocity and energy equations are obtained for the constant properties model with the help of MATHEMATICA software, while for the second model, the solution of the velocity profile is obtained in terms of analytic form with the help of MATHEMATICA version 11.0. The regular perturbation method is selected to solve the energy equation due to its complexity and presented the temperature profile in the form of an approximate analytical solution. In the end, the analytical solutions for total entropy and Bejan number for both cases are obtained with the help of Mathematica version 11.0. A small amount of entropy is observed at the bottom of the channel and maximum entropy is noted at the ciliated walls under the effect of Brinkman number. Maximum value of the entropy number is observed for the case of variable properties as compared to the uniform properties, which showed that the variable liquid properties are the best choice to minimize the entropy of the system and to increase the efficiency of the system.

1. Introduction

The peristaltic flow is an important mechanism, which deals with the area of contraction and expansion of wave occurring along with the walls of the inclined channel. The peristalsis takes place usually in the evolution of bolus through the esophagus, the embryo transfer through the uterine cavity, chyme promotion advancement in the gastrointestinal area, urine flow through the ureter and the vasomotion of blood in vessels. Due to its excessive usage in numerous fields of science, many researchers have been studied the peristaltic transfer under a different arrangement to highlight some modern applications in nuclear industry, such as peristaltic pump, movement of dangerous fluids and heart-lungs machines etc. It is well known that the non-Newtonian liquid is commonly use in the industries and physiology. The analysis on the peristaltic transfer of non-Newtonian fluid has the great interest of the researchers due to its massive applications in medicine and bioengineering.

* Corresponding author at: Institute of Research and Development, Duy Tan University, Da Nang 550000, Viet Nam.
E-mail address: zahraabdelmalek@duytan.edu.vn (Z. Abdelmalek).

https://doi.org/10.1016/j.icheatmasstransfer.2020.104980

Available online 16 October 2020

The Rabinowitsch fluid is a non-Newtonian fluid that can address the complicated physiological functions of the non-Newtonian model and it also depict the features of shear thinning or pseudo plastic (e.g. polymer solutions and blood plasma etc.), shear thickening or dilatant (like, sand and polyethylene glycol etc.) and Newtonian or viscous (e.g. air and water). It is observed that various investigations based on heat transfer analysis have been performed on Rabinowitsch fluid model in wavy channel, inclined channel, curved channel and duct [1–3] under the consideration of uniform and variable liquid properties etc. But no such work has dealt with entropy generation in an inclined ciliated walled channel using Rabinowitsch fluid. The important studies related to peristaltic and cilia motion on the non-Newtonian fluids with the account of entropy generation are cited in the next paragraph.

Ellahi et al. [4] studied the entropy generation in non-Newtonian fluid under the influence of magnetic and slip boundary conditions through the moving plates. Bvp4c MATLAB package was used to numerically solve the set of dimensionless equations. They observed that the value of the Bejan number increased in Dilatant fluid for the different values of the slip parameter. Tripathi and Beg [5] considered two-dimensional channel to analyze the peristaltic flow with nanoparticles under the account of Buongiornio model. They reported the effects of Grashof number, Brownian motion parameter and thermophoresis parameter on the fluid flow, heat transfer and nanoparticles fraction. They concluded that the thermal Grashof number and the bolus size had an inverse relation to each other. Ali et al. [6] analyzed the peristaltic flow of Rabinowitsch fluid in a curved channel. They derived and solved the governing equations without applying symmetric conditions. The velocity was graphically presented for the different values of sundry parameters and it was identified that in an asymmetric channel, streamlines pattern for the given flow was retrieved for large values of radius of the path. Zeeshan et al. [7] considered a wavy channel to discuss the Poiseuille flow suspended by titanium dioxide particles to minimize the entropy generation. They solved the dimensionless equations with the help of the homotopy method and obtained the numerical results by using software package BVPh 2.0. They observed that rise in the values of the electric field parameter resulted in the less energy loss at the middle of the channel. Sheremet et al. [8] reported the computational study of the entropy generation for hot solid blocks by using Tiwari and Das model. They used the finite volume method to solve the dimensionless complex flow equations. They observed that the heat transfer rate increases with the insertion of the nanoparticle in the block. Hayat et al. [9] used the peristaltic flow of the Williamson Nano fluid to minimize the entropy generation in complaint walls of channel under the effect of the magnetic field and Joule heating. No-slip conditions were employed by them in the governing equations of velocity and the temperature. They noted that the slip parameter and the Hartmann number did not affect the temperature of the fluid. Bhatti et al. [10] discussed the effect of thermal radiation and magnetic field on Casson fluid in a metachronal wave. Governing equations were solved with the help of lubrication approximations and represented the motion of fluid, the temperature and the streamlines for the Hartmann number, particle volume fraction, Prandtl number and the Eckert number. They observed that the temperature profile increased versus Prandtl and Eckert numbers. Zeeshan et al. [11] considered the different shapes of the nano-particles in a viscous fluid to investigate the heat and mass transfer over a rotating disk. They considered cylindrical, disk and spherical shapes of the copper nanoparticle with water as base fluid. They presented the results of the entropy generation through pie charts and in tabular form. They observed that the spherical particles are good to minimize the entropy in the system. Bhatti et al. [12] presented a theoretical and a mathematical model for the peristaltic flow of the Nano fluid in a micro channel under the effects of the magnetic field. They employed the perturbation technique to solve the non-linear equations which were obtained by Debby length approximations. They observed that the higher values of the Brinkman number and the magnetic field increased the temperature of the channel. Gibanov et al. [13] numerically examined the natural convection and entropy generation of the ferric oxide nanoparticle with water as base fluid filled in two different porous blocks under the effect of the mag etic field. They observed that the total entropy number diminished by magnetic parameter. Akbar and Nadeem [14] presented the applications of Rabinowitsch fluid model in peristalsis flow. Firstly, they developed the problem and defined the condition of volumetric flow rate then solved and obtained the exact solution of governing equations. They presented the trapping phenomena and plotted the graphs for the velocity with different values of parameter of pseudo-plasticity and flow rate. They concluded that the fluid is Newtonian, pseudo-plastic and dilatant for different values of flow rate. Singh et al. [15] analyzed the effect of the heat transfer on the flow of Rabinowitsch fluid in a channel. They used the approximation of long wavelength and low Reynolds number to examine the cause of heat transfer and peristaltic flow. They obtained the expressions for particle motion, pressure, friction force and heat to discuss them graphically. They concluded that the temperature increases for all types of fluid and size of the trapped bolus decreases with the increase in amplitude ratio. Ramesh et al. [16] discussed the cilia assisted hydromagnetic pumping of bio rheological couple stress fluid in a horizontal wavy channel. MATLAB software was used to solve the system of equations and obtained the solution in analytical form. Their computational results showed that the increasing values of the geometric, material and magnetic control parameters suppressed the pressure of fluid. Shaheen and Nadeem [17] analyzed the production of the metachronal wave of Sisko-fluid in a channel with ciliated walls. They used the homotopy perturbation technique to obtain the solution of the governing equations and showed the graphs of velocity and pressure verses power law index, Weissenberg number and length of cilia tips. Different results were concluded for different values of parameters. They observed that the velocity of the fluid is highest in the middle of the channel while it decreases near the walls of the channel. Vaidya et al. [18] discussed the flow of Rabinowitsch fluid in a porous channel with variable liquid properties. They noted that the consistence of the liquid was dependent on the width of the channel. The perturbation technique was applied to obtain the solution of the governing nonlinear equations. Devaki et al. [19] examined the effects of slip boundary conditions on the flow of Casson fluid with heat transfer in a flexible channel. They concluded that the quantity and size of bolus varies directly with rigidly, stiffness and viscous damping force of the wall. Walika et al. [20] analyzed the curvilinear squeeze film bearing by using Rabinowitsch fluid in a medium of porous walls. Morgan-Cameron approximation was used to obtain the modified equations and solved them analytically. They expressed the pressure distribution and load carrying capacity. Dutta et al. [21] used Weibel's model to analyze the loss of heat in the human lungs. They examined that the heat loss and the Lewis number were inversely proportional to each other for the suitable physical circumstances. Nawaz et al. [22] considered the Soret and Duffour effect to examine the entropy production in a Williamson fluid by applying the magnetic field in a curved channel to present the fluid motion and heat transfer. They observed that the fluid velocity was increased by complaint nature wall while decreased by the damping nature under the effect of different parameters. Kefayati et al. [23] used the Lattice Boltzmann model to discuss the thermal non-Newtonian fluids under the account of porous effects. The applications of Lattice Boltzmann method in the fluid mechanics was reported by Kefayati [24]. Some recent research on the fluid flow with entropy generation and various flow assumptions are listed in Refs. [25–32].

Despite the decent amount of work on this topic, no one has yet studied the minimization of the entropy generation in the flow of Rabinowitsch fluid under the account of constant and variable liquid properties with complaints walls through an inclined channel. In view of this, the main goal of our study is to minimize the entropy generation in Rabinowitsch fluid under the constant and variable liquids properties. Further, to identify the uniform or variable properties are the best

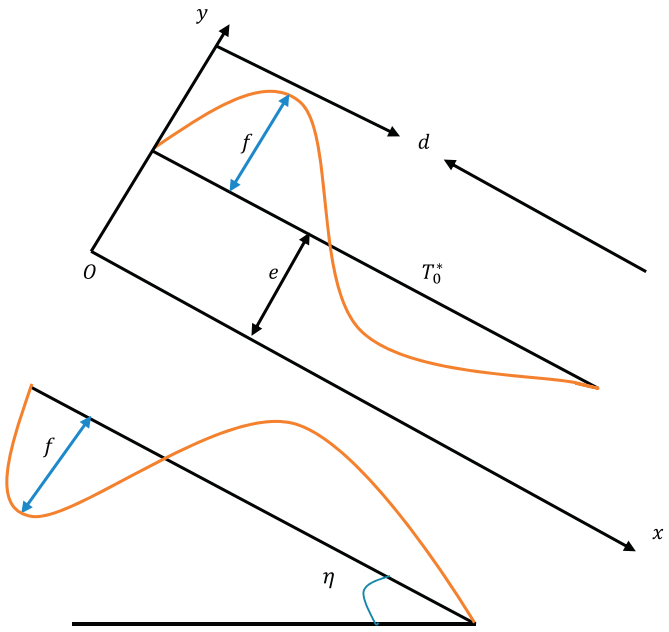

Fig. 1. Schematic diagram of the flow geometry.

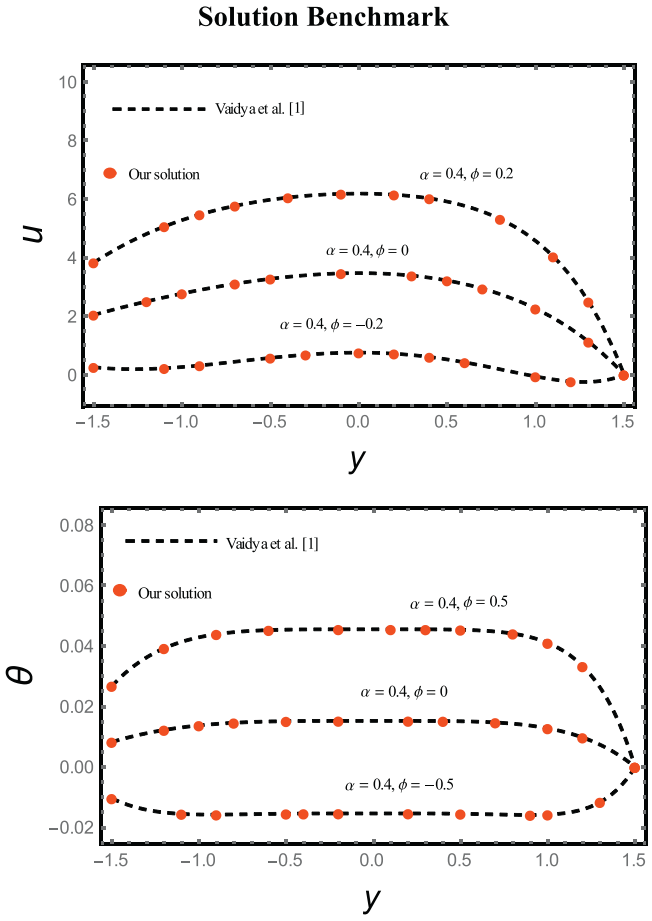

Fig. 2. Comparison with the previous study.

choice to minimize the entropy generation. Since, Rabinowitsch fluid is one of the complex non-Newtonian fluid that exhibits the features of the Pseudo plastic, Dilatant and Newtonian fluids. The comparison of Bejan number for constant and variable properties in Dilatant, Newtonian and Pseudo plastic fluids will also part of our objective. The important results of the study are represented by the graphs under the effect of the different parameters of interest.

2. Problem formulation

Peristalsis of incompressible and viscous Rabinowitsch liquid through an inclined, uniform and symmetrical wavy channel of length l is used for the problem formulation. A travelling wave is produced along the walls of the channel due to liquid flow moving with velocity v. The viscosity and thermal conductivity are taken as constant and variable. These quantities change according to the values of the thickness and temperature. The analysis is carried out for two different models in which constant and variable viscosity and thermal conductivity are considered [1–2]. The physical diagram of the problem is shown in Fig. 1. In Fig. 1, η is the angle of inclination; d denotes the wavelength; T^* is the temperature; e stands for the mean width of the channel and f represents the amplitude.

The stress tensor of Rabinowitsch fluid is defined as [1–2]

$$S_{xy} + \omega_1 S_{xy}^3 = \omega \frac{\partial u_x}{\partial y} \tag{1}$$

In the above equation ω_1 is known as the coefficient of pseudo-plasticity which is used to capture of the characteristic of the fluid, and other quantity ω is called the viscosity of the fluid. The rest of quantities u_x, y and S_{xy} are known as velocity component along $x-axis$, the space coordinate and component of extra stress tensor.

The dimensional of the governing equations in two dimensional time-dependent flow field are given by:

Continuity equation is

$$\frac{\partial u_x}{\partial x} + \frac{\partial u_y}{\partial y} = 0 \tag{2}$$

Equations of motion along x and y direction are given as follow

2.1. Along x-direction

$$\sigma\left(\frac{\partial u_x}{\partial t} + u_x\frac{\partial u_x}{\partial x} + u_y\frac{\partial u_x}{\partial y}\right) = -\frac{\partial q}{\partial x} + \frac{\partial s_{xx}}{\partial x} + \frac{\partial s_{xy}}{\partial y} + \sigma a_g \sin\eta \tag{3}$$

2.2. Along y-direction

$$\sigma\left(\frac{\partial u_y}{\partial t} + u_x\frac{\partial u_y}{\partial x} + u_y\frac{\partial u_y}{\partial y}\right) = -\frac{\partial q}{\partial y} + \frac{\partial s_{xx}}{\partial x} + \frac{\partial s_{xy}}{\partial y} - \sigma a_g \cos\eta \tag{4}$$

Energy equation with viscous dissipation term is

$$\varsigma\sigma\left(\frac{\partial T^*}{\partial t} + u_x\frac{\partial T^*}{\partial x} + u_y\frac{\partial T^*}{\partial y}\right) = \kappa\left(\frac{\partial^2 T^*}{\partial x^2} + \frac{\partial^2 T^*}{\partial y^2}\right) + s_{xx}\frac{\partial u_x}{\partial x} + s_{yy}\frac{\partial u_y}{\partial y} + s_{xy}\left(\frac{\partial u_y}{\partial x} + \frac{\partial u_x}{\partial y}\right) \tag{5}$$

where, u_x and u_y are the velocity components in x and y directions, respectively, a_g denotes the acceleration due to the gravity, σ is the density of the fluid, s_{xx}, s_{xy} and s_{yy}represent the extra stress components, q represents the pressure, ς is the specific heat at constant volume, T^*depicts temperature, κ is the thermal conductivity of the fluid.

For simplicity, we have considered the half width of the channel. In view of this condition, the boundary conditions are given by

$$u_x\,|_{y=l} = 0,\ \frac{\partial u_x}{\partial y}\,|_{y=0} = 0,\ T^*\,|_{y=l} = T_0^*,\ \frac{\partial T^*}{\partial y}\,|_{y=0} = 0 \tag{6}$$

Introducing the non-dimensional parameters as follows

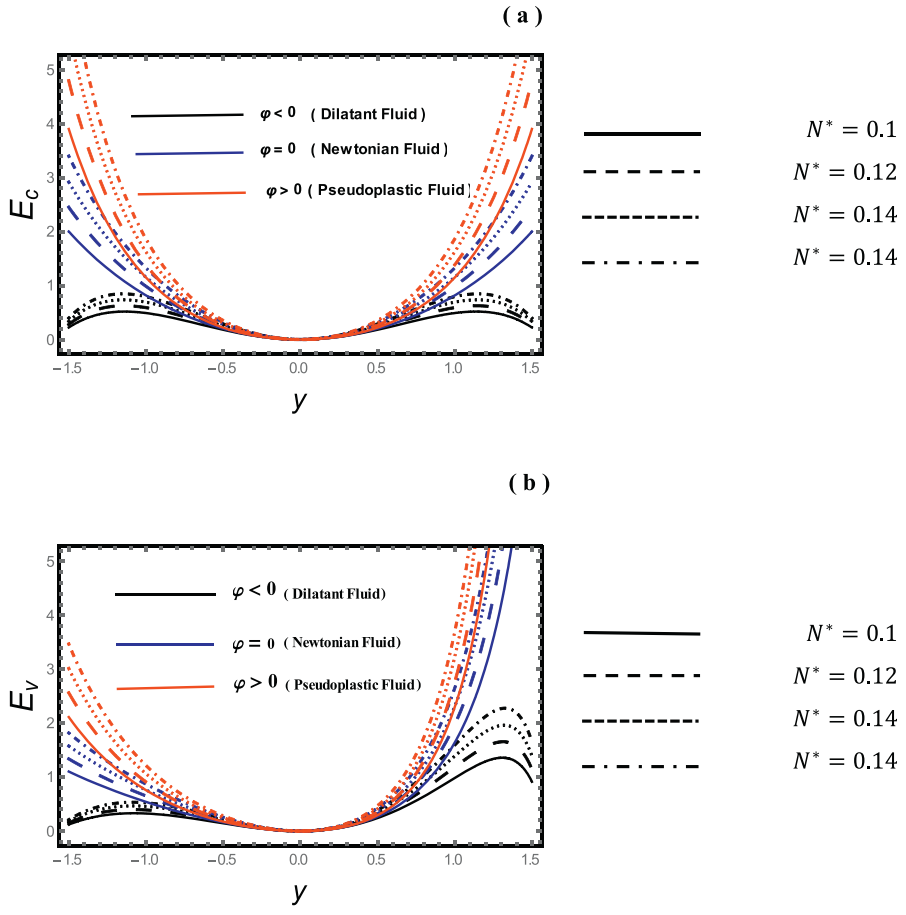

Fig. 3. Effect of Brinkman number (N^*) on the entropy generation (E_C) and (E_V).

$$\bar{x} = \frac{x}{d}, \bar{y} = \frac{y}{e}, \bar{u}_x = \frac{u_x}{v}, \bar{u}_y = \frac{u_y}{v\varsigma}, \bar{q} = \frac{qe^2}{\omega_0 dv}, \bar{s}_{xx} = \frac{s_{xx}e}{\omega_0 v}, \bar{s}_{xy} = \frac{s_{xy}e}{\omega_0 v}, \bar{s}_{yy} = \frac{s_{yy}e}{\omega_0 v}, \bar{l} = \frac{l}{e}, \bar{t} = \frac{t}{e}, F* = \frac{\omega_0 v}{\sigma a_g e^2}, \theta = \frac{T^* - T_0^*}{T_0^*}, \varphi = \frac{\omega_1 v^2 \omega_0^2}{e^2}, \bar{\omega} = \frac{\omega}{\omega_0}, N^* = \frac{ve\omega_0}{T_0^*} \tag{7}$$

The modified form of Eqs. (1)–(5) and boundary conditions (6) are given by

$$\bar{s}_{xy} + \varphi(\bar{s}_{xy})^3 = \bar{\omega}\left(\frac{\partial \bar{u}_x}{\partial \bar{y}}\right) \tag{8}$$

$$\sigma\delta^*\left(\begin{array}{l} v\frac{\partial(\bar{u}_x)}{\partial(\bar{t})} + e\bar{u}_x\frac{\partial(\bar{u}_x)}{\partial(\bar{x})} + \\ \frac{v^2\varsigma^2 d}{e^2}\bar{u}_y\frac{\partial(\bar{u}_x)}{\partial(\bar{y})} \end{array}\right) = \frac{\omega_0 v}{e^2}\left(\begin{array}{l} -\frac{\partial(\bar{q})}{\partial(\bar{x})} + \delta^*\frac{\partial(\bar{s}_{xx})}{\partial(\bar{x})} + \\ \frac{\partial(\bar{s}_{xy})}{\partial(\bar{y})} + \frac{\sigma a_g e^2}{\omega_0 v}\sin\eta \end{array}\right) \tag{9}$$

$$\delta^*\sigma\left(\begin{array}{l} \frac{v^2\varsigma}{e}\frac{\partial(\bar{u}_y)}{\partial(\bar{t})} + v\varsigma\bar{u}_x\frac{\partial(\bar{u}_y)}{\partial(\bar{x})} + \\ \frac{dv^2\varsigma^2}{e^2}\bar{u}_y\frac{\partial(\bar{u}_y)}{\partial(\bar{y})} \end{array}\right) = \frac{\omega_0 dv}{e^3}\left(\begin{array}{l} -\frac{\partial(\bar{q})}{\partial(\bar{y})} + (\delta^*)^2\frac{\partial(\bar{s}_{xx})}{\partial(\bar{x})} + \\ \delta^*\frac{d^2}{e^2}\frac{\partial(\bar{s}_{xy})}{\partial(\bar{y})} - \frac{\cos\eta}{F^*}\delta^* \end{array}\right) \tag{10}$$

$$\varsigma\sigma\delta^*\left(\begin{array}{l} \frac{T_0^* v}{e}\frac{\partial(\theta)}{\partial(\bar{t})} \\ + T_0^*\bar{u}_x\frac{\partial(\theta)}{\partial(\bar{x})} + \\ \frac{\varsigma T_0^* d}{e}u_y\frac{\partial(\theta)}{\partial(\bar{y})} \end{array}\right) = \kappa\frac{T_0^*}{e^2}\left(\begin{array}{l} (\delta^*)^2\frac{\partial^2(\theta)}{\partial(d\bar{x})^2} + \\ \frac{\partial^2(\theta)}{\partial(\bar{y})^2} \end{array}\right) + \left(\begin{array}{l} \left(\frac{v\omega_0}{e}\right)\delta^*\bar{s}_{xx}\frac{\partial(\bar{u}_x)}{\partial(\bar{x})} \\ + \left(\frac{\varsigma v\omega_0 d}{e^2}\right)\delta^*\bar{s}_{yy}\frac{\partial(\bar{u}_y)}{\partial(\bar{y})} \\ + \left(\frac{v\omega_0}{e}\right)\bar{s}_{xy}\left(\delta^*\varsigma\frac{\partial(\bar{u}_y)}{\partial(\bar{x})} + \frac{\partial(\bar{u}_x)}{\partial(\bar{y})}\right) \end{array}\right) \tag{11}$$

$$\bar{u}_{\bar{x}}|_{\bar{y}=\bar{l}} = 0, \left.\frac{\partial \bar{u}_{\bar{x}}}{\partial \bar{y}}\right|_{\bar{y}=0} = 0, \bar{\theta}|_{\bar{y}=\bar{l}} = 0, \left.\frac{\partial \bar{\theta}}{\partial \bar{y}}\right|_{\bar{y}=0} = 0 \tag{12}$$

Under the assumption of long wavelength and small Reynolds number, Eqs. (8)–(12) are given by (for simplicity, we have removed the bars)

$$s_{xy} + \varphi(s_{xy})^3 = \omega\left(\frac{\partial u_x}{\partial y}\right) \tag{13}$$

$$\frac{\partial q}{\partial x} = \frac{\partial S_{xy}}{\partial y} + \frac{sin\eta}{F^*} \tag{14}$$

$$\frac{\partial q}{\partial y} = 0 \tag{15}$$

$$\kappa(\theta)\frac{\partial^2\theta}{\partial y^2} + N^* S_{xy}\frac{\partial u_x}{\partial y} = 0 \tag{16}$$

$$u_x|_{y=l} = 0, \left.\frac{\partial u_x}{\partial y}\right|_{y=0} = 0, \theta|_{y=l} = 0, \left.\frac{\partial \theta}{\partial y}\right|_{y=0} = 0 \tag{17}$$

where $F* = \frac{\omega_0 v}{\sigma a_g e^2}$, $\varphi = \frac{\omega_1 v^2 \omega_0^2}{e^2}$, $N^* = \frac{ve\omega_0}{T_0^*}$

Here we chose viscosity is a linear function of space coordinate y and thermal conductivity is varying linearly with respect to temperature of fluid, and expressions for both properties are defined in the following form [26,29]:

$$\omega(y) = 1 - \beta y \tag{18a}$$

$$\kappa(\theta) = 1 + \alpha\theta \tag{18b}$$

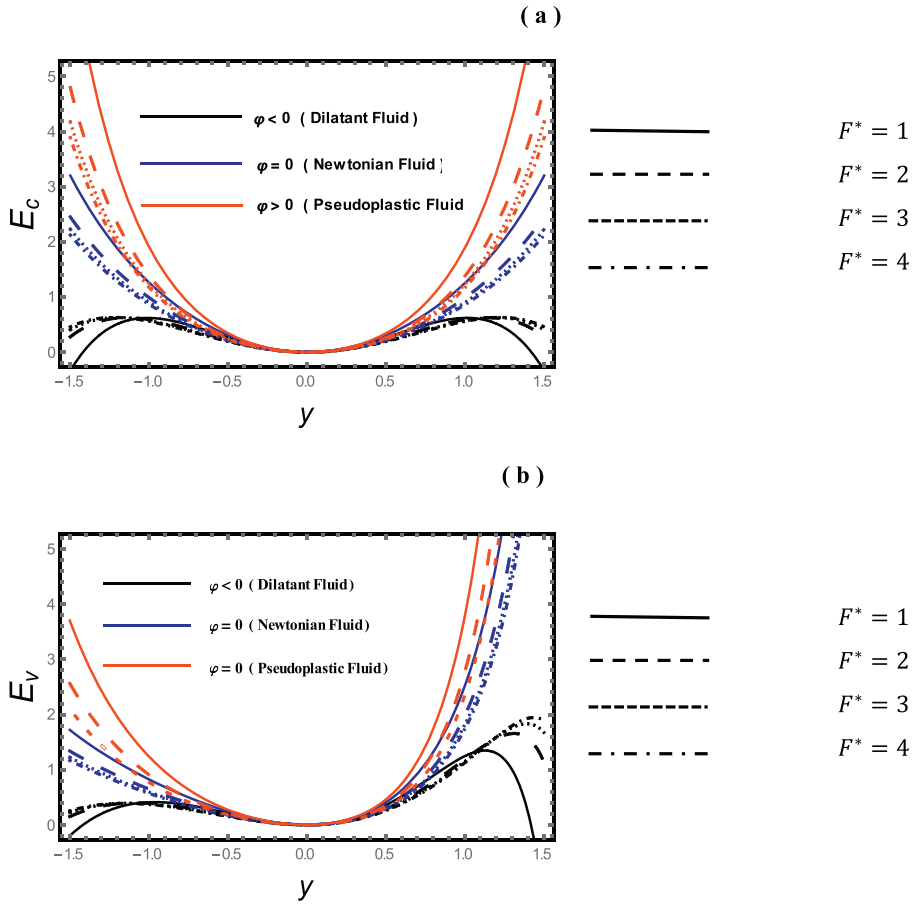

Fig. 4. Effect of body force parameter (F^*) on the entropy generation (E_C) and (E_V).

where β and α are known as the viscosity and thermal conductivity parameters, respectively. When $\alpha \to 0$ and $\beta \to 0$, we get the uniform properties of fluid model.

On solving Eqs. (14) and (16) with boundary conditions Eq. (17), we get

$$S_{xy} = c_1 + y(Q - F_1^*), \text{ where, } Q = \frac{\partial q}{\partial x} \text{ and } F_1^* = \frac{sin\eta}{F^*} \tag{19}$$

$$u = a_0(a_1 + a_2 y + a_3 y^2 + a_4 y^3 + a_5 \log(1 - y\beta)) \tag{20-a}$$

$$\theta = \Lambda_1 + \alpha\begin{pmatrix}\Lambda_2 + y\Lambda_3 + y^2\Lambda_4 + y^3\Lambda_5 + y^4\Lambda_6 + y^5\Lambda_7 \\ + y^6\Lambda_8 + y^7\Lambda_9 + y^8\Lambda_{10} + y^9\Lambda_{11} + y^{10}\Lambda_{12}\end{pmatrix} \tag{20-b}$$

The procedure to obtain the solution of velocity and temperature are given by Vaidya et al. [1]. The quantities a_i and Γ_i are presented in the appendix section.

3. Entropy generation and Bejan number model

The dimensional form of entropy equation is given by

$$Entropy = \kappa(T^*)\left(\frac{\partial T^*}{\partial x} + \frac{\partial T^*}{\partial y}\right)^2 + s_{xx}\frac{\partial u_x}{\partial x} + s_{yy}\frac{\partial u_y}{\partial y} + s_{xy}\left(\frac{\partial u_y}{\partial x} + \frac{\partial u_x}{\partial y}\right) \tag{21}$$

In the presence of the variable viscosity and thermal conductivity, the total entropy is given as follows

$$E_v = \kappa(\theta)\left(\frac{\partial \theta}{\partial y}\right)^2 + \frac{N^*}{\Omega}s_{xy}\frac{\partial u}{\partial y} \tag{22-a}$$

or

$$E_v = (1 + \alpha\theta)\left(\frac{\partial \theta}{\partial y}\right)^2 + \frac{N^*}{\Omega}s_{xy}\frac{\partial u}{\partial y} \tag{22-b}$$

If we let $E_{v_1} = (1 + \alpha\theta)\left(\frac{\partial \theta}{\partial y}\right)^2$ and $E_{v_2} = \frac{N^*}{\Omega}s_{xy}\frac{\partial u}{\partial y}$ then Eq. (22-b) takes the following form

$$E_v = E_{v_1} + E_{v_2} \tag{23}$$

where E_v is called the total entropy number for the case of variable properties. The first and second term in the right hand side of Eq. (23) denotes the entropy generation due to heat transfer and fluid friction, respectively. With the help of Eq. (23), the final expression of total entropy number is given by

$$E_{v_1} = \left(1 + \beta\left(\Lambda_1 + \alpha\begin{pmatrix}\Lambda_2 + y\Lambda_3 + y^2\Lambda_4 \\ + y^3\Lambda_5 + y^4\Lambda_6 + y^5\Lambda_7 \\ + y^6\Lambda_8 + y^7\Lambda_9 + y^8\Lambda_{10} \\ + y^9\Lambda_{11} + y^{10}\Lambda_{12}\end{pmatrix}\right)\right)\left(\alpha\begin{pmatrix}2y\Lambda_4 + 3y^2\Lambda_5 + \\ 4y^3\Lambda_6 + 5y^4\Lambda_7 + \\ 6y^5\Lambda_8 + 7y^8\Lambda_9 + \\ 8y^7\Lambda_{10} + 9y^8\Lambda_{11} + \\ 10y^9\Lambda_{12}\end{pmatrix}\right)^2 \tag{24-a}$$

$$E_{v_2} = \frac{N^*}{\Omega}(y(Q - F_1^*))\left(a_0\begin{pmatrix}a_2 + 2a_3 y + \\ 3a_4 y^2 - \dfrac{a_5\beta}{1 - y\beta}\end{pmatrix}\right) \tag{24-b}$$

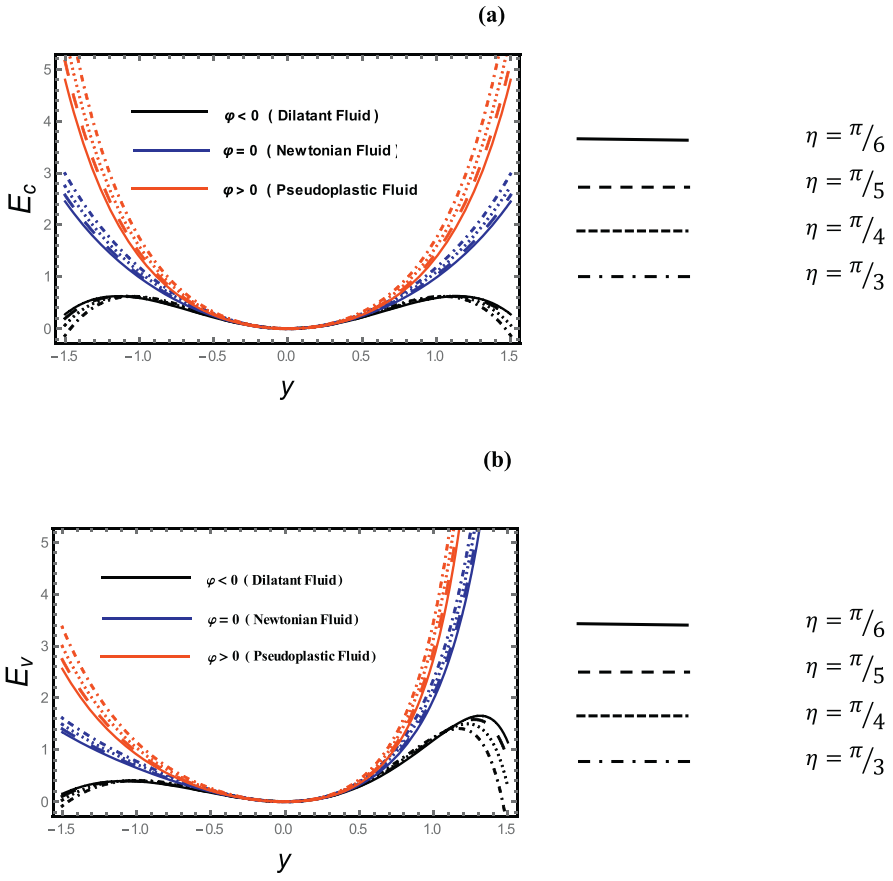

Fig. 5. Effect of inclination angle (η) on the entropy generation (E_C) and (E_V).

$$E_v = \left(\left(1+\beta\left(\Lambda_1+\alpha\begin{pmatrix}\Lambda_2+y\Lambda_3+y^2\Lambda_4\\+y^3\Lambda_5+y^4\Lambda_6+y^5\Lambda_7\\+y^6\Lambda_8+y^7\Lambda_9+y^8\Lambda_{10}\\+y^9\Lambda_{11}+y^{10}\Lambda_{12}\end{pmatrix}\right)\right)\left(\alpha\begin{pmatrix}2y\Lambda_4+3y^2\Lambda_5+\\4y^3\Lambda_6+5y^4\Lambda_7+\\6y^5\Lambda_8+7y^8\Lambda_9+\\8y^7\Lambda_{10}+9y^8\Lambda_{11}+\\10y^9\Lambda_{12}\end{pmatrix}\right)^2\right) + \frac{N^*}{\Omega}(y(Q-F_1^*))\left(a_0\left(\begin{matrix}a_2+2a_3y+\\3a_4y^2-\frac{a_5\beta}{1-y\beta}\end{matrix}\right)\right) \quad (24\text{-c})$$

An irreversibility distribution is evaluated with the help of Bejan number which is denoted by *Be*.This parameter is defined as the ratio of entropy generation due to heat transfer to the total entropy generation. It is defined as

$$(Be)_v = \frac{Entropy\ due\ to\ heat\ and\ mass\ tranfer}{total\ entropy\ of\ the\ system}(Be)_v = \frac{E_{v_1}}{E_v} \quad (25)$$

In the above equation, $(Be)_v$denotes the Bejan number of variable properties. Substituting Eq. (24-a) and (24-c) in Eq. (25), we have

$$\Pi_1 = \left(\left(1+\beta\left(\Lambda_1+\alpha\begin{pmatrix}\Lambda_2+y\Lambda_3+y^2\Lambda_4\\+y^3\Lambda_5+y^4\Lambda_6+y^5\Lambda_7\\+y^6\Lambda_8+y^7\Lambda_9+y^8\Lambda_{10}\\+y^9\Lambda_{11}+y^{10}\Lambda_{12}\end{pmatrix}\right)\right)\left(\alpha\begin{pmatrix}2y\Lambda_4+3y^2\Lambda_5+\\4y^3\Lambda_6+5y^4\Lambda_7+\\6y^5\Lambda_8+7y^8\Lambda_9+\\8y^7\Lambda_{10}+9y^8\Lambda_{11}+\\10y^9\Lambda_{12}\end{pmatrix}\right)^2\right),$$

$$\Pi_2 = \frac{N^*}{\Omega}(y(Q-F_1^*))\left(a_0\left(\begin{matrix}a_2+2a_3y+\\3a_4y^2-\frac{a_5\beta}{1-y\beta}\end{matrix}\right)\right), (Be)_v = \frac{\Pi_1}{\Pi_1+\Pi_2} \quad (26)$$

The values of Bejan number varies from zero to unity. It is clear, for $Be \to 1$ corresponds the irreversibility is dominated due to heat transfer. Secondly, when $Be \to 0$ means the viscous dissipation is dominant. Thirdly, for $Be \to 0.5$, the entropy production is equally produced by both viscous dissipation and heat transfer [22].

The entropy generation and Bejan number for the case of constant properties are obtained for $\alpha \to 0$ and $\beta \to 0$. The calculation of these case is not presented here due to brevity. We denote the entropy and Bejan number with E_c and $(Be)_c$ for the case of constant properties. In this case, we treat viscosity and thermal conductivity taken as constant.

4. Benchmarked solution

Our solution is estimated with the solution obtained by Vaidya et al. [1] for the case of variable liquid properties with complaints walls. These estimations are presented in Fig. 2 (a)–(b) in the form of velocity and temperature for admissible ranges of parameters. In these figures, the dotted lines indicate the solution of Vaidya et al. [1] and slid red circles show our solution. It is noted that our solution and the solution of Vaidya et al. [1] are excellently matched with each other.

5. Results and discussion

In this section, we shall explain the effect of Brinkman number (N^*), body force parameter (F^*), the angle of inclination (η) and temperature difference parameter (Ω) on the entropy generation and the Bejan number for both the constant and the variable liquid properties of Rabinowitch fluid model. This non-Newtonian fluid model is well established model and suitable for an extensive range of shear rates i.e. 0 to $10^6/s$ [1]. Moreover, the thermal conductivity of the fluid behaves a linear function of temperature between the ranges of 0^0 to 400^0 [2]. For this, we chose two different cases. In the first case, we discussed the entropy and Bejan numbers for variable properties and second case with constant properties, respectively. For the better understanding of

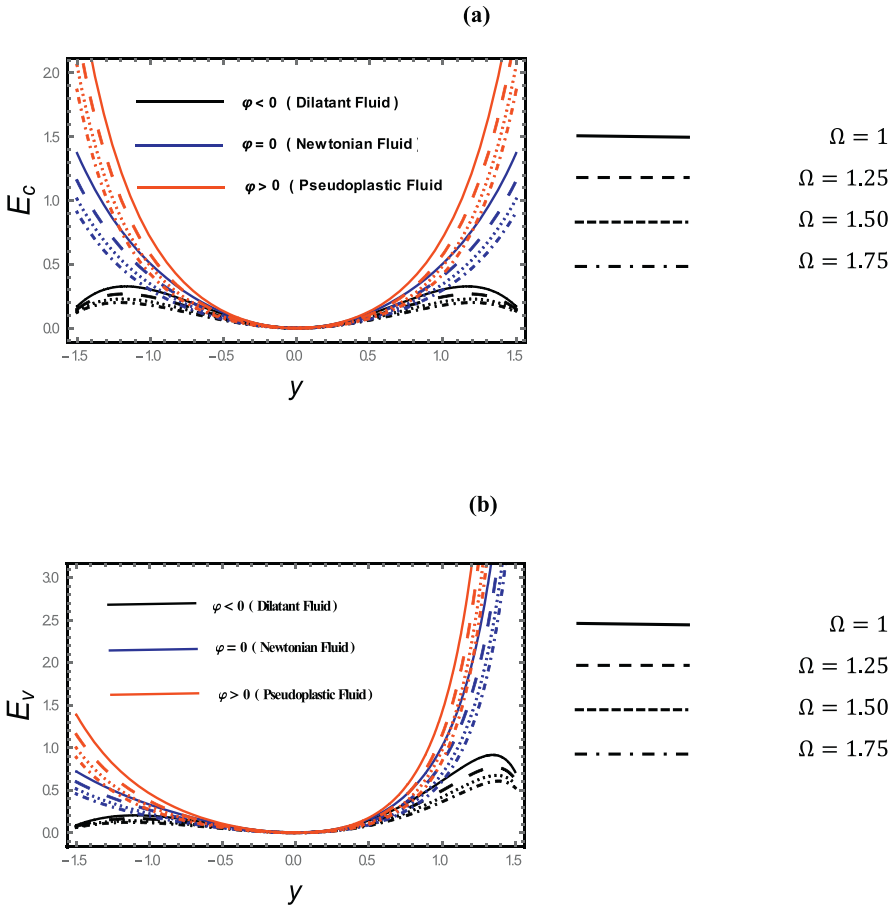

Fig. 6. Effect of temperature difference parameter (Ω) on the entropy generation (E_C) and (E_V).

the given analysis, we assign the different notation to entropy and Bejan number of variable and constant properties. For this, we assign $(E)_v$ and $(E)_c$ to the variable and constant entropy generations. For Bejan number we use $(Be)_v$ and $(Be)_c$ to differentiate the Bejan number of variable and constant liquid properties, respectively. In the first case, we chose the viscosity and thermal conductivity as a variable in which viscosity is taken as a function of temperature. On the other hand, we chose viscosity and thermal conductivity are constant. These flow phenomena are discussed for three different types of fluids namely, Dilatant, Newtonian and Pseudo plastic fluids. Authors developed four figures to show the physical behavior of entropy generation for different physical parameters and construct four tables to present the values of Bejan number via non-dimensional parameters.

The graphical representation of the effect of the pertinent parameters on the entropy is given by Figs. (3–6) are for the Dilatant ($\varphi < 0$), Newtonian ($\varphi = 0$) and the pseudoplastic fluids ($\varphi > 0$). Here, we have chosen the comparative study for both the constant and the variable properties in order to express the results in a better way. The effects of Brinkman number on entropy generation for the case of variable and constant liquid properties are shown in Fig. 3 (a)–(b). From these figures, it is observed that the entropy generation increases with increase in the values of Brinkman number for the case of shear thickening, Newtonian and shear thinning fluids. The physical reason is that when we increase the value of Brinkman number the heat transfer rate enhances the viscosity of the fluid as a result, the entropy generation increases. Further, the small amount of entropy is noted at the bottom of the channel and maximum entropy is recorded at both the ciliated walls of the channel. From both figures, we observed that the value of the entropy number is maximum for the case of variable properties as compared to uniform properties which means that variable properties are good choice to minimize the entropy of the system. Fig. 4 (a)–(b) reported the effects of body force parameter on entropy generation for both considered cases. It is observed that the body force parameter and entropy generation have an inverse relation with each other on both the ciliated walls. The body force parameter reduces the entropy of the system for both cases. Fig. 5 (a)–(b) depicts the results for the entropy (E_c) and the entropy (E_v) under the effects of the angle of inclination with admissible range of inclination angle $\eta(\eta = \pi/6, \pi/5, \pi/4, \pi/3)$ for$\varphi < 0, \varphi = 0$ *and* $\varphi > 0$, respectively. These figures reveal that the entropy of the system in ciliated wall enhances in the increment of inclination angles. On the other hand, the temperature difference parameter suppressed the entropy generation (see Figs. 6 (a) & (b)). The reason is that when we increase the temperature difference parameter, the friction in the fluid particles decreases due diminishing the fluid's viscosity.

5.1. Trapping phenomenon

The stream function ψ is calculated with the help of the following expression [1]

$$u = \frac{\partial \Psi}{\partial y} \tag{27}$$

Figs. 7 (a)–(d), 8 (a)–(d) and 9 (a)–(f) highlights the behavior of trapped bolus due to the relevant parameters. Figs. 7 (a)–(c) and 8 (a)–(c) represent the behavior of variable viscosity and angle of inclination on the trapped bolus. It is seen that the behavior of variable viscosity is opposite to that of angle of inclination because the size of the trapped bolus increases with the increase in the variable viscosity and decreases for the larger values of angle of inclination. The effect of

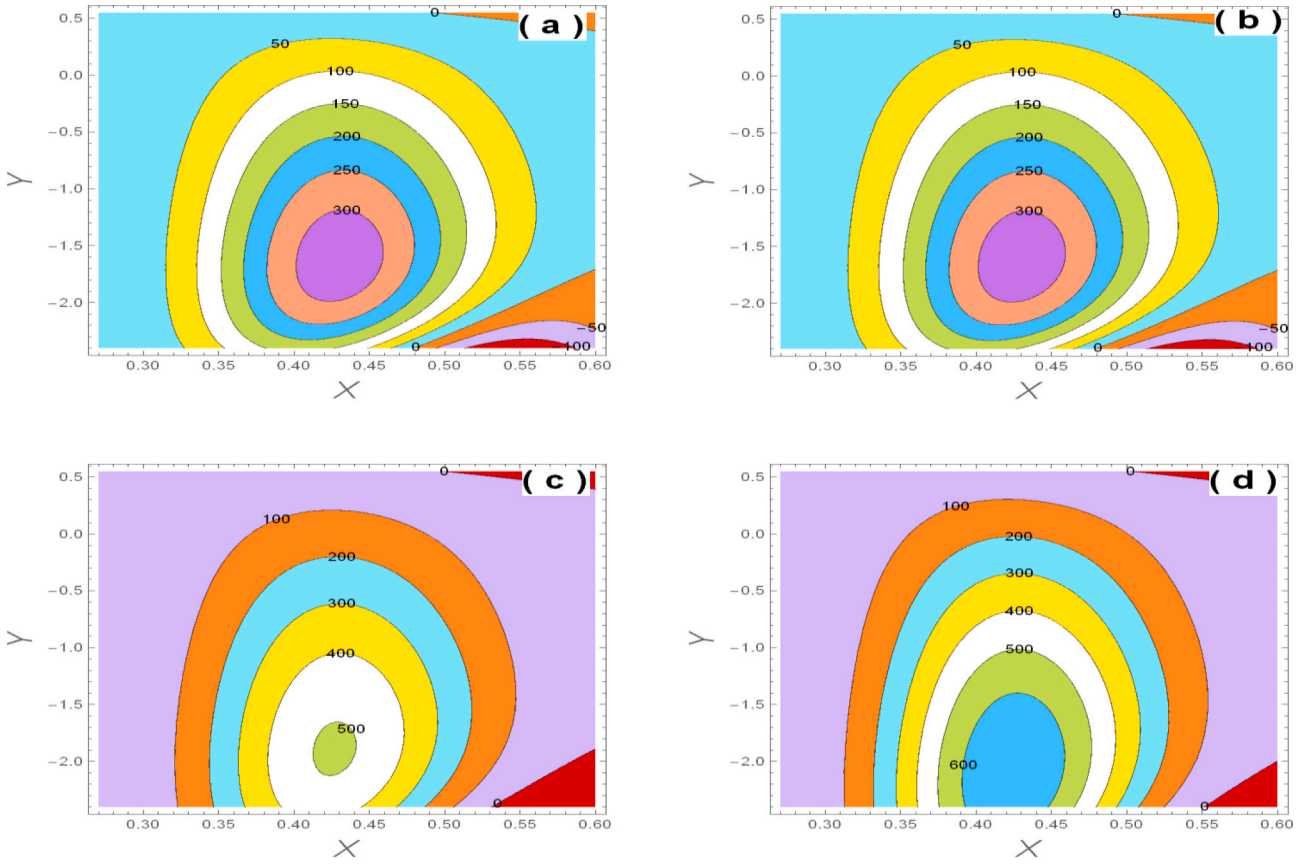

Fig. 7. (a–d): Streamlines for the co-efficient of variable viscosity (Ω = 0.1, 0.2, 0.3, 0.4).

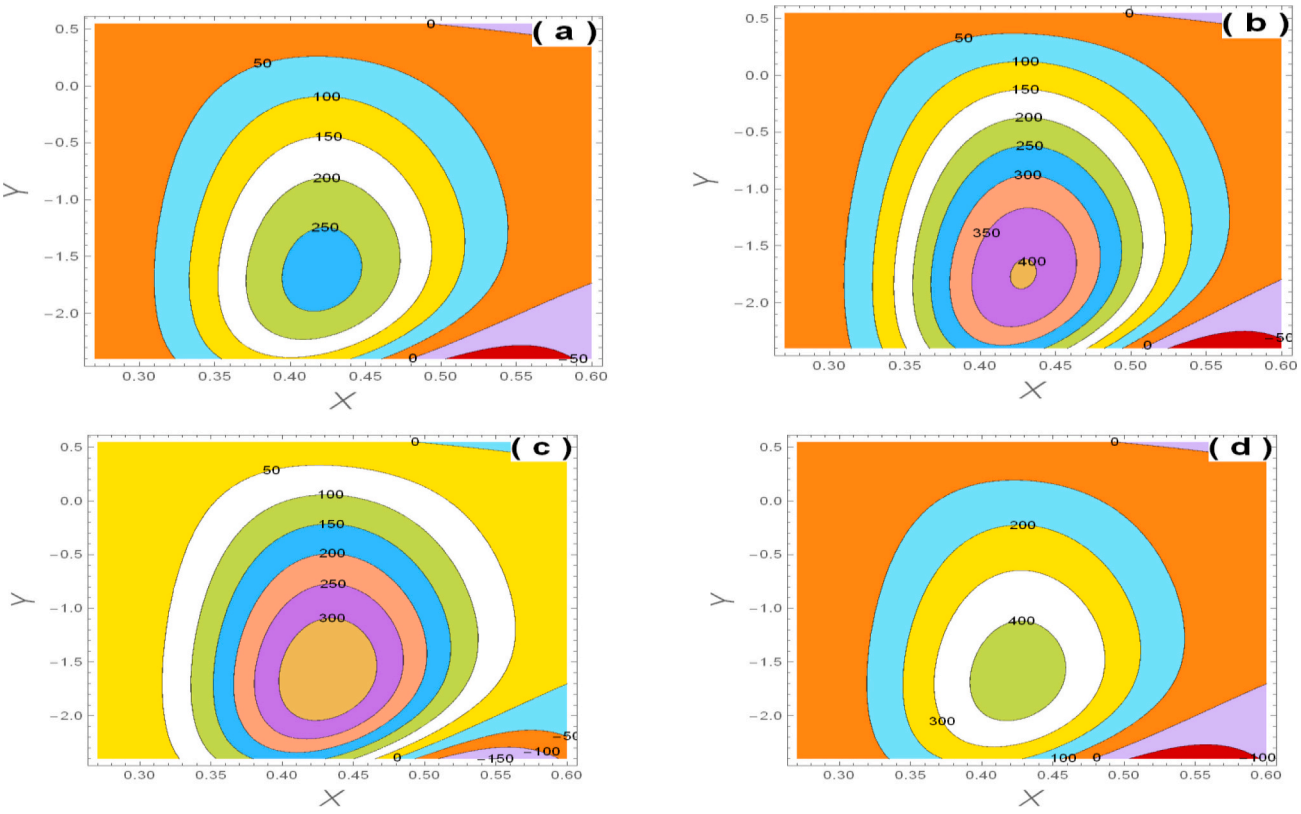

Fig. 8. (a–d): Streamlines for angle of inclination (η).

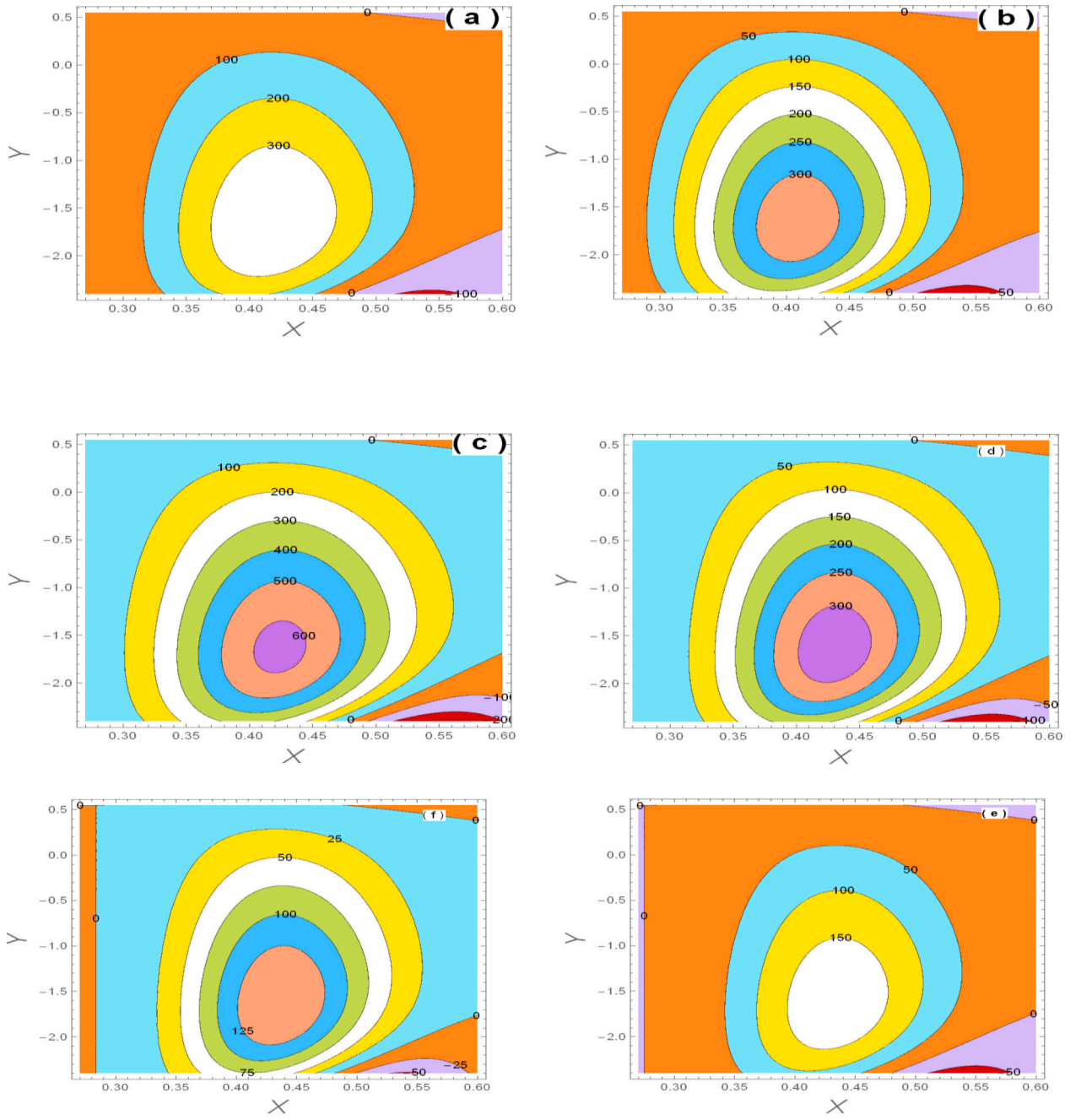

$$J_1 = 0.09, J_2 = 0.04, J_3 = 0.4, J_4 = 0.002, J_5 = 0.01$$
$$J_1 = 0.1, J_2 = 0.04, J_3 = 0.4, J_4 = 0.002, J_5 = 0.01$$
$$J_1 = 0.1, J_2 = 0.042, J_3 = 0.4, J_4 = 0.002, J_5 = 0.01$$
$$J_1 = 0.1, J_2 = 0.042, J_3 = 0.45, J_4 = 0.002, J_5 = 0.01$$
$$J_1 = 0.1, J_2 = 0.042, J_3 = 0.45, J_4 = 0.0022, J_5 = 0.01$$
$$J_1 = 0.1, J_2 = 0.042, J_3 = 0.45, J_4 = 0.0022, J_5 = 0.04$$

Fig. 9. (a–f): Effect of wall tension parameter (J_1), mass characterizing parameter (J_2), wall damping parameter (J_3), wall rigidity parameter (J_4) and wall elastic parameter (J_5) on Streamlines.

Table 1
Variation of Bejan number versus Brinkman number for constant and variables properties.
($x = 0.2$, $t_0 = 0.1$, $F = 2$, $\epsilon = 0.6$, $\eta = \frac{\pi}{6}$, $h = 1.5$, $\Omega = 0.5$, $J_1 = 0.1$, $J_2 = 0.04$, $J_3 = 0.4$, $J_4 = 0.002$, $J_5 = 0.01$).

N^*	$\alpha = \beta = 0$			$\alpha = 0.5, \beta = 0.5$		
	$(B_C)_{max}$			$(B_V)_{max}$		
	$\phi < 0$	$\phi = 0$	$\phi > 0$	$\phi < 0$	$\phi = 0$	$\phi > 0$
0.1	0.2223	0.1012	0.1119	0.2148	0.15206	0.1965
0.2	0.3638	0.1838	0.2013	0.3536	0.2640	0.3285
0.3	0.4618	0.2525	0.2743	0.4507	0.3498	0.4232
0.4	0.5336	0.3106	0.3351	0.5225	0.4177	0.4946
0.5	0.5885	0.3602	0.3865	0.5776	0.4728	0.5502

Table 2
Variation of Bejan number versus body force parameter for constant and variables properties.
($x = 0.2$, $t_0 = 0.1$, $\epsilon = 0.6$, $\eta = \frac{\pi}{6}$, $N^* = 0.2$, $h = 1.5$, $\Omega = 0.5$, $J_1 = 0.1$, $J_2 = 0.04$, $J_3 = 0.4$, $J_4 = 0.002$, $J_5 = 0.01$).

F^*	$\alpha = \beta = 0$			$\alpha = 0.5, \beta = 0.5$		
	$(B_C)_{max}$			$(B_V)_{max}$		
	$\phi < 0$	$\phi = 0$	$\phi > 0$	$\phi < 0$	$\phi = 0$	$\phi > 0$
1	−0.4025	0.2218	0.2670	−0.2038	0.3122	0.3998
2	0.3638	0.1838	0.2013	0.3536	0.2640	0.3285
3	0.2711	0.1714	0.1966	0.2689	0.2478	0.3050
4	0.2309	0.1652	0.1918	0.2453	0.2397	0.2934
5	0.1682	0.1616	0.1764	0.2339	0.2348	0.2865

Table 3
Variation of Bejan number versus angle of inclination for constant and variables properties. ($x = 0.2$, $t_0 = 0.1$, $F = 2$, $\epsilon = 0.6$, $N^* = 0.2$, $h = 1.5$, $\Omega = 0.5$, $J_1 = 0.1$, $J_2 = 0.04$, $J_3 = 0.4$, $J_4 = 0.002$, $J_5 = 0.01$).

η	$\alpha = \beta = 0$			$\alpha = 0.5, \beta = 0.5$		
	$(B_C)_{max}$			$(B_V)_{max}$		
	$\phi < 0$	$\phi = 0$	$\phi > 0$	$\phi < 0$	$\phi = 0$	$\phi > 0$
$\pi/6$	0.3638	0.18383	0.2013	0.3536	0.2640	0.3285
$\pi/5$	0.5104	0.1904	0.2325	0.4522	0.2725	0.3410
$\pi/4$	0.9279	0.1995	0.2349	0.9111	0.2841	0.3580
$\pi/3$	−1.1736	0.2116	0.2441	−0.7852	0.2994	0.3807
$\pi/2$	−0.4025	0.2218	0.2670	−0.2038	0.3122	0.3998

ψ_1, ψ_2, ψ_3, $\psi_4$and ψ_5 on the trapped bolus is explained in Fig. 9 (a)–(f). It is noticed that for the increasing values of ψ_1, ψ_2 and ψ_4, the size of the bolus decreases while increases for ψ_3 and ψ_5.

Now, we are going to explain the maximum values of Bejan number for both constant and variable liquids properties under the effects of the pertinent parameters on Dilatant, Newtonian and pseudo plastic fluids by Tables 1–4. These tables are showing that the value of Bejan number increases versus Brinkman number, angle of inclination and temperature difference parameter while an opposite behavior is highlighted against the body force parameter. These tables are also predicting the maximum values of Bejan number for the variable liquid properties. Moreover, Dilatant fluid is showing the higher profile of Bejan number as compared to Pseudo-Plastic and Newtonian one.

6. Conclusions

Entropy generation analysis of Rabinowitsch fluid under the effects of complaints walls inside an inclined channel are investigated here. Two cases are presented here based on constant and variable liquid properties. In the first case, the viscosity and thermal conductivity are taken as a variable while in the second case, both these quantities are taken as constant, respectively. The exact solution of velocity equation is obtained while the perturbation method is used to find the solution of heat equation for the case of variable liquid properties while the exact

Table 4
Variation of Bejan number versus for temperature difference parameter for constant and variables properties.
$x = 0.2$, $t_0 = 0.1$, $F = 2$, $\epsilon = 0.6$, $\eta = \frac{\pi}{6}$, $N^* = 0.2$, $h = 1.5$, $J_1 = 0.1$, $J_2 = 0.04$, $J_3 = 0.4$, $J_4 = 0.002$, $J_5 = 0.01$.

Ω	$\alpha = \beta = 0$			$\alpha = 0.5, \beta = 0.5$		
	$(B_C)_{max}$			$(B_V)_{max}$		
	$\phi < 0$	$\phi = 0$	$\phi > 0$	$\phi < 0$	$\phi = 0$	$\phi > 0$
1.00	0.5335	0.3106	0.3351	0.5225	0.4177	0.4946
1.25	0.5884	0.3602	0.3865	0.5776	0.4728	0.5502
1.50	0.6318	0.4032	0.4305	0.6214	0.5183	0.5948
1.75	0.6668	0.4408	0.4686	0.6569	0.5566	0.6313
2.00	0.6958	0.4739	0.5020	0.6863	0.5893	0.6618

solution for velocity and temperature equations is presented with the help of symbolic software. The important findings of this investigation are highlighted as follows:

- The profile of entropy generation is minimizing for the case of variable liquid properties as compare to uniform properties.
- The values of Bejan number are higher for Dilatant fluid and minimum in the case of a Newtonian fluid.
- The variable liquid properties are best choice to minimize the entropy generation, i.e. we achieved the goal to guess which case is beneficial to increase the efficiency of the system.
- The Bejan number and entropy generation are showing the increasing behavior verses inclination angle, Brinkman number and temperature difference parameter while an opposite trend is noted via body force parameter.
- In the presented analysis, we have neglected the effects of thermal radiation, heat generation and magnetic field (i.e. neglecting the electrically conducting properties) which have important applications in biomedical engineering. These suggest an interesting area for future analysis.

Declaration of Competing Interest

Authors have no conflict of interest related to this manuscript.

Acknowledgement

The research was supported by the National Natural Science Foundation of China (Grant Nos. 11971142, 11871202, 61673169, 11701176, 11626101, 11601485).

Appendix A. Appendix

$$a_0 = \frac{1}{6\beta^4}(Q - F_1^*),\ a_1 = \begin{pmatrix} 6l\beta^3 + lQ^2\beta(6 + l\beta(3 + 2l\beta))\varphi \\ + 6(\beta^2 + Q^2\varphi)\log(1 - l\beta) + \\ \varphi\begin{pmatrix} l\beta(6 + l\beta(3 + 2l\beta)) + \\ 6\log(1 - l\beta) \end{pmatrix} F_1^*(-2Q + F_1^*) \end{pmatrix} a_2 = \begin{pmatrix} -6\beta^3 - 6Q^2\beta\varphi + \\ 12Q\beta\varphi F_1^* - 6\beta\varphi(F_1^*)^2 \end{pmatrix},\ a_3 = \begin{pmatrix} -3Q^2\beta^2\varphi + 6Q\beta^2\varphi F_1^* \\ -3\beta^2\varphi(F_1^*)^2 \end{pmatrix} a_4$$

$$= \begin{pmatrix} -2Q^2\beta^3\varphi + 4Q\beta^3\varphi F_1^* \\ -2\beta^3\varphi(F_1^*)^2 \end{pmatrix}$$

$$a_5 = \begin{pmatrix} -6\beta^2 - 6Q^2\varphi + \\ 12Q\varphi F_1^* - 6\varphi(F_1^*)^2 \end{pmatrix}$$

$$b_1 = a_0N^*(F_1^* - Q),\ b_2 = -\frac{a_5}{\beta},\ b_3 = \frac{a_5}{2},\ b_4 = \frac{a_2}{6},\ b_5 = \frac{a_3}{6},\ b_6 = \frac{3a_4}{20},\ b_7 = -\frac{a_5}{\beta^2},\ b_8 = \frac{a_5}{\beta},\ b_9$$

$$= \frac{1}{2}b_1\begin{pmatrix} l(b_1l(b_2 + l(b_3 + l(b_4 + l(b_5 + b_6l))))^2 + \\ 2b_0(l(b_3 + l(b_4 + l(b_5 + b_6l))) + b_7\beta)) + \\ (b_7 + b_8l)\log[1 - l\beta]\begin{pmatrix} 2\begin{pmatrix} b_0 + b_1l\begin{pmatrix} b_2 + l\begin{pmatrix} b_3 + \\ l(b_4 + l(b_5 + b_6l)) \end{pmatrix} \end{pmatrix} \end{pmatrix} \\ + b_1(b_7 + b_8l)\log[1 - l\beta] \end{pmatrix} \end{pmatrix},\ b_{10} = -b_0b_1b_7,\ b_{11} = -\frac{1}{2}b_1{}^2b_7{}^2,\ b_{12} = -b_0b_1b_7\beta,\ b_{13} = \begin{pmatrix} -b_1{}^2b_2b_7 \\ -b_0b_1b_8 \end{pmatrix},\ b_{14}$$

$$= -b_1{}^2b_7b_8,\ b_{15} = \begin{pmatrix} -\frac{1}{2}b_1{}^2b_2{}^2 \\ -b_0b_1b_3 \end{pmatrix},\ b_{16} = \begin{pmatrix} -b_1{}^2b_3b_7 \\ -b_1{}^2b_2b_8 \end{pmatrix},\ b_{17} = -\frac{1}{2}b_1{}^2b_8{}^2,\ b_{18} = \begin{pmatrix} -b_1{}^2b_2b_3 \\ -b_0b_1b_4 \end{pmatrix},\ b_{19} = \begin{pmatrix} -b_1{}^2b_4b_7 \\ -b_1{}^2b_3b_8 \end{pmatrix},\ b_{20} = \begin{pmatrix} -\frac{1}{2}b_1{}^2b_3{}^2 - b_1{}^2b_2b_4 \\ -b_0b_1b_5 \end{pmatrix},$$

$$b_{21} = \begin{pmatrix} -b_1{}^2b_5b_7 \\ -b_1{}^2b_4b_8 \end{pmatrix},\ b_{22} = \begin{pmatrix} -b_1{}^2b_3b_4 - b_1{}^2b_2b_5 \\ -b_0b_1b_6 \end{pmatrix},\ b_{23} = \begin{pmatrix} -b_1{}^2b_6b_7 \\ -b_1{}^2b_5b_8 \end{pmatrix},\ b_{24} = \begin{pmatrix} -\frac{1}{2}b_1{}^2b_4{}^2 - b_1{}^2b_3b_5 \\ -b_1{}^2b_2b_6 \end{pmatrix},$$

$$b_{25} = -b_1{}^2b_6b_8,\ b_{26} = \begin{pmatrix} -b_1{}^2b_4b_5 \\ -b_1{}^2b_3b_6 \end{pmatrix},\ b_{27} = \begin{pmatrix} -\frac{1}{2}b_1{}^2b_5{}^2 \\ -b_1{}^2b_4b_6 \end{pmatrix},\ b_{28} = -b_1{}^2b_5b_6,\ b_{29} = -\frac{1}{2}b_1{}^2b_6{}^2,$$

$$\Lambda_1 = \begin{pmatrix} b_0 + b_1\begin{pmatrix} b_2y + b_3y^2 + b_4y^3 + b_5y^4 \\ + b_6y^5 + b_7\log(1 - y\beta) \\ + b_8y\log(1 - y\beta) \end{pmatrix} \end{pmatrix},\ \Lambda_2 = \begin{pmatrix} b_9 + b_{10}\log(1 - y\beta) + \\ b_{11}\log(1 - y\beta)^2 \end{pmatrix},\ \Lambda_3 = \begin{pmatrix} b_{12} + b_{13}\log(1 - y\beta) + \\ b_{14}\log(1 - y\beta)^2 \end{pmatrix},\ \Lambda_4 = \begin{pmatrix} b_{15} + b_{16}\log(1 - y\beta) + \\ b_{17}\log(1 - y\beta)^2 \end{pmatrix},\ \Lambda_5$$

$$= (b_{18} + b_{19}\log(1 - y\beta)),$$

$$\Lambda_6 = (b_{20} + b_{21}\log(1 - y\beta)),\ \Lambda_7 = (b_{22} + b_{23}\log(1 - y\beta)),\ \Lambda_8 = (b_{24} + b_{25}\log(1 - y\beta)),$$

$$\Lambda_9 = b_{26},\ \Lambda_{10} = b_{27},\ \Lambda_{11} = b_{28},\ \Lambda_{12} = b_{29}$$

$$Q = \frac{\partial q}{\partial x},\ F_1^* = \frac{\sin\eta}{F^*},\ F^* = \frac{v\omega_0}{\sigma a_g e^2},\ N^* = \frac{ve\omega_0}{T_0^*},\ \varphi = \omega_1\frac{v^2{\omega_0}^2}{e^2}$$

Credit author statement

Component of the research Author's number, substantial contribution to conception and design Mubbashar Nazeer, substantial contribution to acquisition of data Waqas Ali, substantial contribution to analysis and interpretation of data Zareen Zafar, revised drafting the article Yu-Ming Chu

and Seifefine Kadry, critically revising the article for important intellectual content M. Ijaz Khan and Zahra Abdelmalek, final approval of the version to be published by All authors.

References

[1] H. Vaidya, C. Rajashekhar, G. Manjunatha, K.V. Prasad, Peristaltic mechanism of a Rabinowitsch fluid in an inclined channel with complaint wall and variable liquid properties, J. Br. Soc. Mech. Sci. Eng. 41 (1) (2019) 52–60.

[2] R. Sarawana, K. Vajravelu, S. Sreenadh, Influence of complaint walls and heat transfer on the peristaltic transport of a Rabinowitsch fluid in an Inclined Channel, Zeitschrift fü Naturforschung 73 (9) (2018) 1–13.

[3] E.N. Maraj, S. Nadeem, Application of Rabinowitsch fluid model for the mathematical analysis of peristaltic flow in a Curved Channel, Math. Biosci. 70 (7) (2015) 513–520.

[4] R. Ellahi, S.Z. Alamir, A. Basit, A. Majeed, Effects of MHD and slip on heat transfer boundary layer flow over a moving plate based on specific entropy generation, J. Taibah Univ. Sci. 12 (4) (2018) 476–482.

[5] D. Tripathi, O.A. Beg, A study on peristaltic flow of nano-fluids: applications in drug delievery system, Int. J. Heat Mass Transf. 70 (1) (2014) 61–70.

[6] N. Ali, M. Sajid, K. Javid, R. Ahmed, Peristaltic flow of Rabinowitsch fluid in a curved channel: mathematical analysis revisited, Zeitschrift fü Naturforschung A 72 (3) (2016) 245–251.

[7] A. Zeeshan, N. Shehzad, T. Abbas, R. Ellahi, Effects of radioactive electro-magneto hydrodynamics diminishing internal energy of pressure driven flow of titanium dioxide water nanofluid due to entropy generation, Entropy 21 (3) (2019) 236–249.

[8] M.A. Sheremet, H.F. Oztop, I. Pop, N. Abu-Hamedeh, Analysis of entropy generation in natural convection of nano fluids inside a square cavity having hot solid block: Tiwari and das model, Entropy 18 (1) (2015) 1–9.

[9] T. Hayat, S. Nawaz, A. Alsaedi, O. Mahian, Entropy generation in peristaltic flow of Willianson nano-fluid, Phys. Scr. 94 (12) (2019) 1–18.

[10] M.M. Bhatti, A. Zeeshan, R. Ellahi, Heat transfer with thermal radiation on MHD particle fluid suspension induced by metachronal wave, Pramana J. Phys. 89 (3) (2017) 1–9.

[11] A. Zeeshan, M. Hassan, R. Ellahi, M. Nawaz, Shape effect of nano size particles in un-steady mixed convection flow of nano fluid over disk with entropy generation, Aust. J. Mech. Eng. 231 (4) (2016) 1–9.

[12] M.M. Bhatti, A. Zeeshan, R. Ellahi, Heat transfer with thermal radiation on MHD particle fluid suspension induced by metachronal wave, Pramana J. Phys. 89 (1) (2017) 1–13.

[13] Gibanov, N. S., Shermet, M. A, Oztop, H. F., & Saleem, K. (2017). MHD natural convection and entropy generation in open cavity having different horizontal porous blocks saturated with ferro fluid. J. Magn. Magn. Mater. 452(1), 193–204.

[14] N.S. Akbar, S. Nadeem, Applications of Rabinowitsch fluid model in peristalsis, Zeitschrift fur Naturforschung A J. Phys. Sci. 69 (8–9) (2014) 473–480.

[15] U.P. Singh, A. Medhavi, R.S. Gupta, S.S. Bhatt, Theoretical study of heat transfer on peristaltic transport of non-Newtonian fluid flowing in a channel: Rabinowitsch fluid model, J. Math. Eng. Manag. Sci. 3 (4) (2018) 450–571.

[16] K. Ramesh, D. Tripathi, O.A. Beg, Cilia assisted hydro magnetic pumping of bio rheological couple stress fluids, Propuls. Power Res. 8 (3) (2019) 221–233.

[17] A. Shaheen, S. Nadeem, Metachronal wave analysis for non-Newtonian fluid inside a symmetric channel with ciliated walls, Respir. Physiol. 7 (1) (2017) 1536–1549.

[18] H. Vaidya, R. Choudhry, M. Gudekote, K.V. Prasad, Effect of variable liquid properties on peristaltic transport of Rabinowitsch liquid on convectively heated complaint porous, J. Cent. South Univ. 26 (1) (2019) 1116–1132.

[19] P. Devaki, S. Sreenadth, K. Vajravelu, K.V. Prasad, H. Vaidya, Wall properties and slip consequences on peristaltic transport of casson liquid in a flexible channel with heat transfer, Appl. Math. Non Linear Sci. 3 (1) (2018) 277–290.

[20] A. Walika, E. Walicki, Jurczak, & Falicki, J., Curvilinear squeeze film bearing with porous wall lubricated by a Rabinowitsch fluid, Int. J. Appl. Mech. Eng. 22 (2) (2017) 427–441.

[21] A. Dutta, H. Chattopadhay, H. Yasmin, M. Rhimi-Gorji, Entropy generation in the human lungs due to the effect of psychrometri condition and friction in the respiratory tract, Comput. Methods Prog. Biomed. 180 (1) (2019) 1–12.

[22] S. Nawaz, T. Hayat, A. Alsaedi, Analysis of entropy generation in peristalsis of Williamson fluid in curved channel under radial magnetic field, Comput. Methods Prog. Biomed. 180 (1) (2019) 1–13.

[23] G. Kefayati, H. Tang, H.A. Chan, X. Wang, A lattice Boltzmann model for thermal non-Newtonian fluid flows through porous media, Comput. Fluids 176 (2018) 224–244.

[24] G. Kefayati, An immersed boundary-lattice Boltzmann method for thermal and thermo-solutal problems of Newtonian and non-Newtonian fluids, Phys. Fluids 32 (2020) 073103.

[25] M.I. Khan, F. Alzahrani, A. Hobiny, A. Ali, Fully developed second order velocity slip Darcy-Forchheimer flow by a variable thicked surface of disk with entropy generation, Int. Commun. Heat Mass Transf. 117 (2020) 104778.

[26] M. YuKruKsoy, M. Pakdemirli, Approximate analytical solutions for the flow of a third-grade fluid in a pipe, Int. J. Non Linear Mech. 37 (2002) 187–195.

[27] R. Muhammad, M.I. Khan, N.B. Khan, M. Jameel, Magnetohydrodynamics (MHD) radiated nanomaterial viscous material flow by a curved surface with second order slip and entropy generation, Comput. Methods Prog. Biomed. 189 (2020) 105294.

[28] R. Muhammad, M.I. Khan, M. Jameel, N.B. Khan, Fully developed Darcy-Forchheimer mixed convective flow over a curved surface with activation energy and entropy generation, Comput. Methods Prog. Biomed. 188 (2020) 105298.

[29] A.T. Akinshilo, O. Olaye, On the analysis of the Erying Powell model based fluid flow in a pipe with temperature dependent viscosity and internal heat generation, J. King Saud Univ. Eng. Sci. 31 (2019) 271–279.

[30] M.I. Khan, M. Waqas, T. Hayat, A. Alsaedi, A comparative study of Casson fluid with homogeneous-heterogeneous reactions, J. Colloid Interface Sci. 498 (2017) 85–90.

[31] M.I. Khan, S. Qayyum, T. Hayat, M.I. Khan, A. Alsaedi, T.A. Khan, Entropy generation in radiative motion of tangent hyperbolic nanofluid in presence of activation energy and nonlinear mixed convection, Phys. Lett. A 382 (2018) 2017–2026.

[32] S. Qayyum, M.I. Khan, T. Hayat, A. Alsaedi, A framework for nonlinear thermal radiation and homogeneous-heterogeneous reactions flow based on silver-water and copper-water nanoparticles: a numerical model for probable error, Respir. Physiol. 7 (2017) 1907–1914.